Petroleum Science 19 (2022) 1174–1184

Contents lists available at ScienceDirect

Petroleum Science

journal homepage: www.keaipublishing.com/en/journals/petroleum-science

Original Paper

Characteristics and mechanisms of supercritical CO_2 flooding under different factors in low-permeability reservoirs

Zheng Chen [a, b], Yu-Liang Su [a, b, *], Lei Li [a, b], Fan-Kun Meng [c], Xiao-Mei Zhou [a, b]

[a] School of Petroleum Engineering, China University of Petroleum (East China), Qingdao, 266580, Shandong, PR China
[b] Key Laboratory of Unconventional Oil & Gas Development (China University of Petroleum (East China)), Ministry of Education, Qingdao, 266580, Shandong, PR China
[c] School of Petroleum Engineering, Yangtze University, Wuhan, 430100, Hubei, PR China

ARTICLE INFO

Article history:
Received 10 August 2021
Accepted 21 December 2021
Available online 22 January 2022

Edited by Yan-Hua Sun

Keywords:
Low-permeability reservoir
Supercritical CO_2 flooding
Influence mechanism
Enhanced oil recovery
Injection capacity

ABSTRACT

In recent years, supercritical CO_2 flooding has become an effective method for developing low-permeability reservoirs. In supercritical CO_2 flooding different factors influence the mechanism of its displacement process for oil recovery. Asynchronous injection–production modes can use supercritical CO_2 to enhance oil recovery but may also worsen the injection capacity. Cores with high permeability have higher oil recovery rates and better injection capacity, however, gas channeling occurs. Supercritical CO_2 flooding has a higher oil recovery at high pressure levels, which delays the occurrence of gas channeling. Conversely, gas injection has lower displacement efficiency but better injection capacity at the high water cut stage. This study analyzes the displacement characteristics of supercritical CO_2 flooding with a series of experiments under different injection and production parameters. Experimental results show that the gas breakthrough stage has the fastest oil production and the supercritical CO_2 injection capacity variation tendency is closely related to the gas–oil ratio. Further experiments show that higher injection rates represent significant ultimate oil recovery and injection index, providing a good reference for developing low-permeability reservoirs.

1. Introduction

As the total global demand for oil continues to increase, the output of proven conventional oil reservoirs cannot meet the needs of consumption growth, and the contradiction between supply and demand has become increasingly prominent. This will inevitably require people to continue to explore unconventional oil reservoirs (Chen et al., 2021; Dong et al., 2020; Pei et al., 2020). Reasonably exploiting this type of oil reservoir plays an important role in the development of the petroleum industry (Zhao et al., 2020a). Low-permeability reservoirs have tight lithology and small particles and exhibit low porosity and low permeability. The most commonly used development method is water injection. However, the high starting pressure and high remaining oil content make it difficult to effectively implement water flooding in low-permeability reservoirs (Fang et al., 2019b; Fan et al., 2015; Shi et al., 2017; Wang et al., 2014; Hu et al., 2018). Therefore, gas injection becomes an effective method to enhance oil recovery after water flooding. The density of supercritical carbon dioxide is close to that of liquid, and it has the characteristics of good injection performance and low viscosity (Wang et al., 2018; Li et al., 2006; Xiong et al., 2015). In the context of global warming, CO_2 flooding is recognized as one of the most potent methods for enhancing oil recovery (Fang et al., 2019a; Wei et al., 2021; Zhao et al., 2015) and mitigating the greenhouse environment problem at the same time. In recent years, it has been widely used in the development of major unconventional oil fields. Field tests of CO_2 flooding have shown that it is easier to inject CO_2 in low-permeability reservoirs than water. CO_2 flooding can increase oil recovery by 10% over water flooding. The reservoir also provides a good area for carbon dioxide storage (Cheng et al., 2017).

Core flooding experiments and numerical simulation methods are effective approaches to investigate the characteristics of CO_2 flooding (Sander et al., 2017; Sun et al., 2016). There are few studies of supercritical CO_2 using numerical simulation methods, which

* Corresponding author. School of Petroleum Engineering, China University of Petroleum (East China), Qingdao, 266580, Shandong, PR China.
E-mail address: suyuliang@upc.edu.cn (Y.-L. Su).

https://doi.org/10.1016/j.petsci.2022.01.016
1995-8226/

mainly focus on using commercial software and self-built mathematical models to simulate the flow process and variation characteristics of various parameters of supercritical CO_2 in the displacement process (Cui et al., 2011; Zhang et al., 2020; Zhu et al., 2016). At present, many scholars still take experimental means to understand the displacement characteristics of supercritical CO_2. It is believed that the permeability of a low permeability reservoir can be improved by injecting supercritical CO_2 first by adjusting injection and production parameters and injection methods. Meanwhile, the influence of gravity effect in immiscible flooding cannot be ignored (Bikkina et al., 2016; Han et al., 2016; Wang et al., 2011). However, the oil samples used in their studies are single hydrocarbon compounds, and the rock samples used are generally short cores, and only one factor is considered to affect the supercritical CO_2 displacement behavior. Given the above problems, Li et al. (2018) studied the oil-increasing laws of various supercritical CO_2 displacement methods by using long cores and live oil. They believe that the miscible flooding has the minimum injection pressure difference and the maximum recovery factor, and the supercritical CO_2 alternating water-miscible flooding has a lower injection pressure and smaller gas and oil production. At the same time, they also believe that the increase in gas-oil ratio does not represent a breakthrough of supercritical CO_2, and gas injection at high water cut stage has a lag in water content change (Li et al., 2018). In subsequent studies, the influences of pressure, supercritical CO_2 content, soaking time, and permeability on supercritical CO_2 displacement characteristics were studied successively. However, the rock samples and oil samples used were short core and degassed oil, which differed greatly from the actual reservoir conditions (Chen et al., 2018; Li et al., 2019b; Xu et al., 2020).

In view of the strong heterogeneity of low-permeability reservoirs, Park et al. (2017) studied the influence of core sedimentary heterogeneity and displacement pressure difference on CO_2 flooding (Park et al., 2017). They revealed that the capillary pressure difference caused by core heterogeneity is one of the main reasons for the CO_2 displacement characteristics. At the same time, many scholars also use the experimental method of assembling cores of different permeability into parallel or vertical combination samples to study the CO_2 flooding effect under different injection-production parameters (Al-Bayati et al., 2019; Wang et al., 2021; Wei et al., 2014).

The above studies discussed the characteristics of supercritical CO_2 flooding at the macro scale of the core. Some scholars evaluated water flooding and supercritical CO_2 flooding in core flooding experiments by combining CT scanning experiment and nuclear magnetic resonance experiment with macro core experiment. Thus, the saturation and fluid distribution changes of porous cores under typical reservoir temperature and pressure conditions are clarified (Qian et al., 2020; Mahabadi et al., 2020; Zhao et al., 2020b). At the same time, to study the details of pore-scale flow patterns in the porous media that cannot be resolved, some microsimulation methods are used to study and understand the dynamic displacement process of carbon dioxide injection in porous media, for example the Boltzmann method (Liu et al., 2014, 2020; Yamabe et al., 2015).

All previous studies have shown that gas channeling and low oil recovery under supercritical CO_2 flooding of low permeability cores are inevitable (Shen et al., 2021; Wang et al., 2019; Zhang et al., 2012). It is necessary to study the characteristics and mechanisms of supercritical CO_2 flooding under different factors. However, as shown in Table 1, for most of the published studies, the experimental design is focused on one kind of influencing factor. The rock samples used are short cores, and the gas breakout and interflow occurred earlier during gas injection flooding, so it is difficult to accurately reflect the seepage parameters during the displacement process. The oil sample is a mixture of degassed oil or other decanes, and the influence of the original gas-oil ratio of formation oil and the change of degassed oil composition is not considered. In general, there are few reports on the study of supercritical CO_2 displacement characteristics by using long core and live oil. Therefore, it is necessary to carry out supercritical CO_2 flooding long core experiments to comprehensively analyze the displacement characteristics and influence mechanism of supercritical CO_2 on live oil under different injection and production parameters.

In this study, the live oil configuration and inspection method are independently designed to ensure the matching of the gas-oil ratio and the stability of live oil. At the same time, the supercritical CO_2 flooding experiment is carried out using natural outcrop long cores in low-permeability reservoirs. This paper studies and discusses various parameters that affect CO_2 displacement efficiency, gas channeling characteristics, and inject capacities, such as reservoir physical properties, formation conditions, and injection-production system. This paper uses long core samples and live oil, which is closer to reservoir conditions than previously reported. Based on these discussions, we try to clarify the influence mechanism of different factors on the characteristics of CO_2 flooding.

2. Experimental

2.1. Experimental materials

The core samples are outcrop cores, with their basic parameters shown in Table 2. Permeability was determined by a standard measuring method of 99.99% pure nitrogen, while porosity was determined by the liquid weighing method. The purity of CO_2 gas used in the experiment was 99.99%. The live oil sample used for core saturation was based on the composition of the gas sample provided by the oilfield, original gas–oil ratio, and crude oil viscosity. The oil properties are shown in Table 3. Distilled water was used in the experiment, while the influence of salinity on the core was ignored.

2.2. Procedures of testing

The schematic of the extended core displacement experiment device is shown in Fig. 1. A Vindum pump provides driving power and a confining pressure pump provides confining pressure and back pressure. Confining pressure, back pressure, and inlet pressure were measured using pressure gauges. The volumetric cylinder, shown in Fig. 1, was used to measure the liquid volume. The gas volume was measured by discharging sodium carbonate solution by gas.

The block studied in this research is block G of the Shengli Oilfield in China. The original reservoir pressure and temperature are 42.6 MPa and 126 °C. The development in recent years has caused a decrease in reservoir pressure to the current value of 19.0 MPa. The experimental temperature was set at 50 °C, higher than the critical temperature of carbon dioxide. The experimental back pressure was set at the current reservoir pressure of 20 MPa, ensuring that the injected CO_2 was in a supercritical state. The experimental steps mainly included core processing and displacement as follows.

(1) According to the crude oil characteristic data given by the oil field, live oil was configured by a sample mixing device. Based on the original gas–oil ratio data provided by the oilfield, the required gas and dead oil were calculated. Then, the dead oil, gas, and a small amount of kerosene were mixed in the sample mixing equipment to fully dissolve the gas in crude oil.

Table 1
Summary of experimental research on CO_2 flooding.

Author	Year	Experimental scale	Rock sample	Oil sample	Research factors
Wang et al.	2011	Core scale	/	/	Injection rate
Bikkina et al.	2016	Core scale	Short cores	*n*-hexadecane	Wetting
Han et al.	2016	Core scale	Sandstone plate	Normal decane	Gravity effect
Park et al.	2017	Core scale	Short cores	*i*-decane	Heterogeneity
Li et al.	2018	Core scale	Long cores	Live oil	Displacement modes
Chen et al.	2018	Core scale	Short cores	Gas-free oil	CO_2 content and pressure
Li et al.	2019	Core scale	Short cores	Separator oil	Injection pressure, soaking time, and core permeability
Zhu et al.	2020	Pore scale	Micromodel	Gas-free oil	Injection pressure
Zhao et al.	2020	Core scale	Short cores	*n*-decane	Displacement medium
Xu et al.	2020	Core scale	Short cores	/	Effective confining pressure

Table 2
The basic parameters of core samples.

Core No.	Diameter, mm	Length, mm	Permeability, mD	Porosity, %
1	25	200	8.1	17.4
2	25	200	5.8	16.8
3	25	200	5.2	16.6
4	25	200	5.1	16.3
5	25	200	5.6	16.3
6	25	200	5.8	16.5
7	25	200	7.5	17.1
8	25	200	7.0	17.1
9	25	200	8.0	17.3
10	25	200	2.5	16.0
11	25	200	5.6	16.3
12	25	200	7.8	17.2
13	25	200	8.2	17.5
14	25	200	0.63	15.8
15	25	200	5.4	16.8

(2) A portion of live oil was extracted and measured separately in liquid and gas volumes. The relative error between actual and theoretical gas–oil ratio was calculated and controlled within 10% to check whether the gas in live oil firmly dissolves. The relative error between the actual gas–oil ratio and the live gas–oil ratio was 6.38%.

(3) A part of the live oil was then introduced into the viscometer to measure its viscosity before calculating its relative error with respect to the viscosity of the actual formation crude oil to control it within 10% (Table 3). Suppose the configured live oil properties are different from the actual, repeat steps (1)–(3) to reconfigure the oil. The viscosity of the live oil was 2.55 mPa·s and the relative error was 3.66%.

(4) The live oil that meets the standard was pressure-maintained and exported to the accumulator. A pressure tank was used for real–time pressure monitoring of the export process.

(5) The outcrop core was cleaned and dried before measuring the permeability of the core using the gas measurement method. The porosity of the cores was measured by saturating the cores with distilled water. The results are shown in Table 2.

(6) The prepared live oil was injected into the water-saturated cores with a backpressure of 13 MPa. The irreducible water saturation was calculated by flooding with a displacement pressure of 20 MPa until no water flowed out at the end of the core.

(7) Supercritical CO_2 flooding was conducted on oil-bearing cores under different factors. The experimental design parameters are shown in Table 4. The injection methods were divided into three types: continuous gas injection (CGI), synchronous injection (SI), and asynchronous injection-

Table 3
Live oil properties.

Formation oil viscosity, mPa·s	Formation oil density, g/cm^3	Degassed oil density, g/cm^3	Volume factor	Dissolved gas-oil ratio, m^3/m^3	Bubble point pressure, MPa
2.46	0.79	0.87	1.144	37.6	10.18

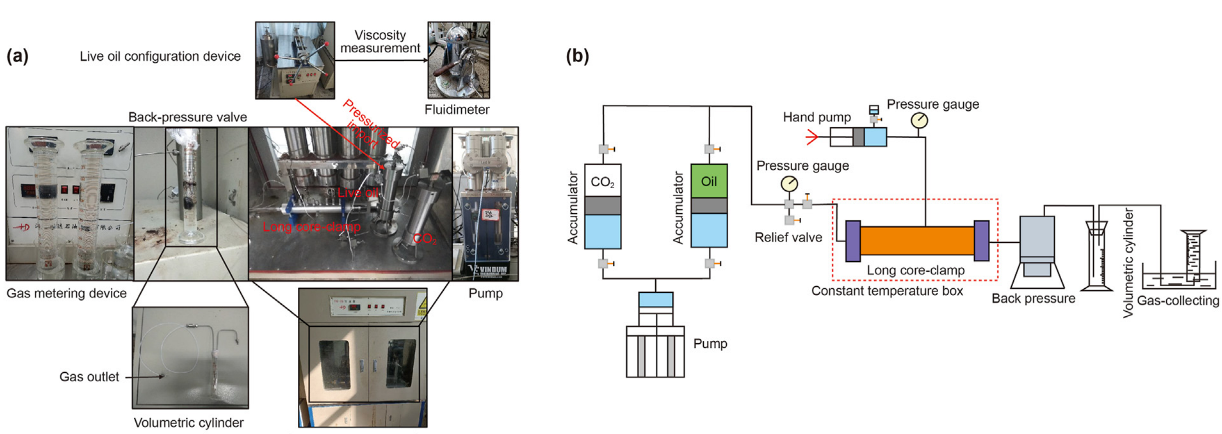

Fig. 1. Experimental setup for supercritical CO_2 displacement: (**a**) experimental device; (**b**) schematic diagram.

Table 4
The operation parameters for different cases.

Core No.	Permeability, mD	Initial injection pressure, MPa	Injection rate, mL/min	Injection mode	Back pressure, MPa	Water saturation, %	Research factors
3	5.2	20	0.1	CGI	20	41.68	Injection rate
11	5.6	20	0.05	CGI	20	43.11	
15	5.4	20	0.5	CGI	20	40.55	
7	7.5	20	0.01	AIP	20	46.36	Injection–production modes
8	7.0	20	0.01	AIP	20	37.42	
12	7.8	20	0.01	SI	20	40.75	
4	5.1	20	0.01	CGI	20	43.73	Permeability
10	2.5	20	0.01	CGI	20	36.31	
14	0.63	20	0.01	CGI	20	36.79	
1	8.1	20	0.01	CGI	20	41.43	Back pressure
9	8.0	30	0.01	CGI	30	41.09	
13	8.2	10	0.01	CGI	10	38.85	
2	5.8	20	0.01	CGI	20	42.00	Water saturation
5	5.6	20	0.01	CGI	20	60.00	
6	5.8	20	0.01	CGI	20	80.00	

production (AIP). Section 3.2 describes the schemes of synchronous and AIP.

3. Results and discussion

The experimental methods in Section 2 analyze the oil displacement characteristics under different injection rates, injection–production modes, permeability, pressure levels, and water saturation. This section discusses the influence mechanisms of different factors of supercritical CO_2 flooding in low-permeability reservoirs by comparing the recovery factor, gas–oil ratio, and injection capacity under various factors.

3.1. Displacement characteristics at different injection rates

The recovery of each stage at different injection rates is shown in Fig. 2. The oil recovery rate rises slowly before the gas breakthrough at three different injection rates. In this stage, CO_2 dissolves in crude oil, reducing the viscosity of crude oil and improving the fluidity ratio. When supercritical CO_2 breaks through at the end of the core, the dynamic balance among the original CO_2, crude oil, and water is broken due to the decrease in pressure, forming the three-phase flow of oil, gas, and water. At this point, gas begins to appear at the end of the core. This stage depicts maximum oil production due to the carrying effect of supercritical CO_2 on crude oil during the breakthrough. Compared with low injection rate, the stable production stage of high injection rate becomes more extended, which leads to an increase in final recovery (Ajoma et al., 2021; He et al., 2019; Li et al., 2019a). However, the recovery efficiency before the breakthrough at the gas injection rate of 0.1 mL/min is more significant than that at 0.5 mL/min, proving the optimal value. Fig. 3 shows that the gas–oil ratio rises sharply with the increase in injection volume, while the gas forms a controlled channel. The utilization degree of crude oil by the subsequent injection of CO_2 decreases sharply, and the recovery degree no longer increases. When the injection rate is 0.05 mL/min, the final oil recovery is 80%. Likewise, with the injection rate of 0.1 mL/min, the final oil recovery is 88.42%, and with the injection rate of 0.5 mL/min, the final oil recovery is 92.86%. The higher the core pressure level and increase in injection rates, the more fully miscible supercritical CO_2 and crude oil, resulting in more significant oil recovery. The increase in the injection rate can prolong gas channeling occurrence (Matkivskyi et al., 2021), as shown in Fig. 3. The first occurrence of gas channeling is when the gas injection rate is 0.05 mL/min. When the gas injection rate is 0.05 mL/min, the gas channeling occurs before the gas injection rate is 0.1 mL/min, proving that gas channeling can be delayed by increasing the gas injection rate. Still, it cannot increase indefinitely because the increased range has an optimal value.

The injection index was introduced to evaluate the injection capacity to facilitate the analysis of the injection capacity during the supercritical CO_2 flooding process. The meaning of injection index is the volume of gas injected per unit time under unit pressure difference, which can be expressed as follows.

$$I = \frac{60 v_i}{P_2 - P_1} \tag{1}$$

where I is the gas injection index, v_i is the injection rate, P_2 is the inlet pressure, and P_1 is the back pressure.

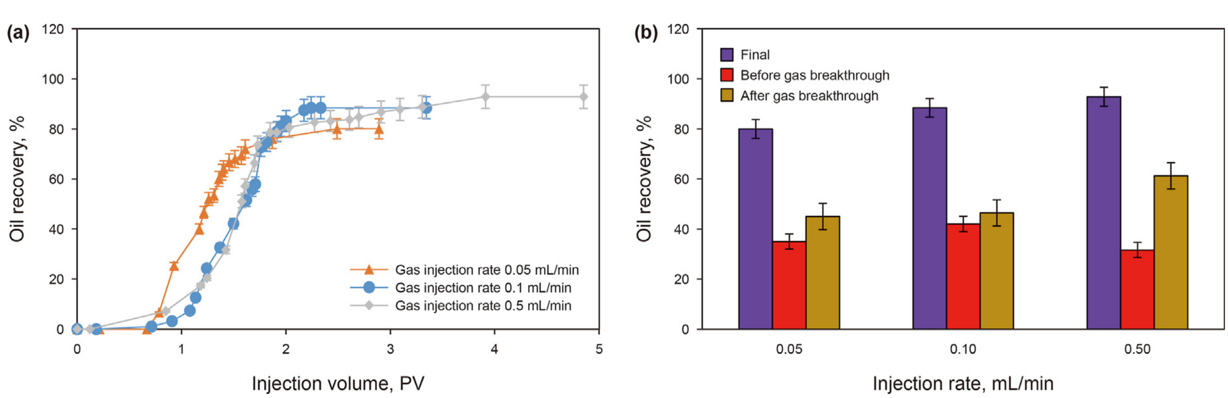

Fig. 2. Relationship between oil recovery and injection volume (**a**) and gas injection rate (**b**).

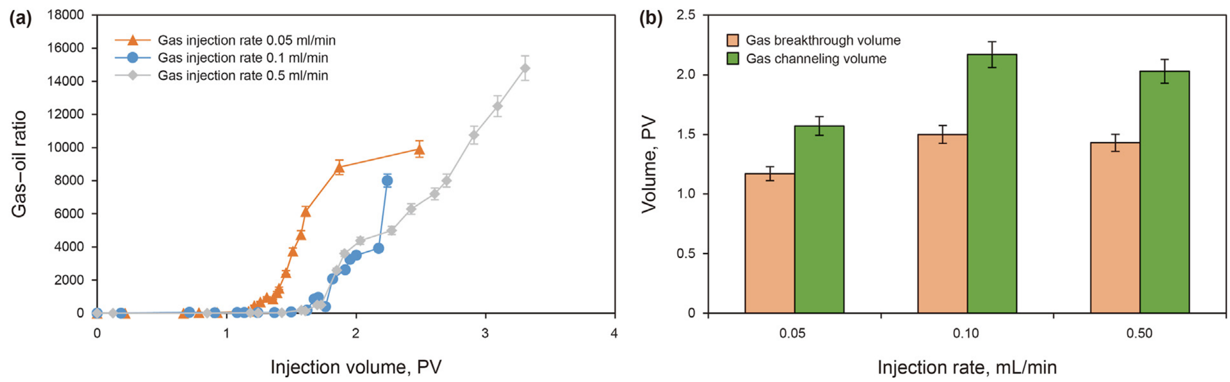

Fig. 3. Curves of gas–oil ratio versus injection volume (**a**), and injection volumes occurring gas breakthrough and gas channeling (**b**) at different gas injection rates.

The variation tendency of the injection index at different injection rates is shown in Fig. 4. As the injection rate increases, the inlet pressure increases to a certain extent, but this is not a sign of poor injection capability. It can be understood that the higher the injection rate before the occurrence of gas channeling, the larger the injection index, proving a better injection capability. In the initial injection stage, the injection index was higher. This is because the initially injected supercritical CO_2 is easily dissolved in the crude oil, resulting in better injection capacity. After gas channeling occurs, the injection index increases sharply due to the formation of gas channels in the core. At this time, the supercritical CO_2 can be easily injected.

3.2. Displacement characteristics of different injection-production modes

In order to study the displacement characteristics of different injection–production modes, three injection–production modes were designed. In Mode 1, supercritical CO_2 was continuously injected into the cores at an injection rate of 0.01 mL/min. In Mode 2, the outlet was closed for initial injection and opened after 0.5 PV of supercritical CO_2 was injected. The injection rate was kept at 0.01 mL/min in Mode 2. In Mode 3, the outlet was initially opened, 0.25 PV of supercritical CO_2 was injected at an injection rate of 0.01 mL/min, and then the outlet was closed. After injecting another 0.25 PV, the outlet was opened.

The recovery rates at different stages under different injection and production methods are shown in Fig. 5. The oil displacement

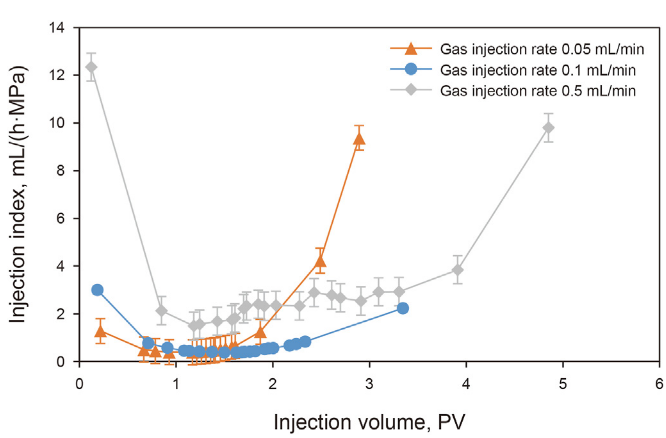

Fig. 4. Comparison of injection index at different injection volumes and gas injection rates.

efficiency of Mode 1 increases rapidly. However, the increased rate of the flooding efficiency of Mode 2 and Mode 3 after the soaking process is faster than that of Mode 1. After the injection and production coupling adjustment, the recovery rate before gas breakthrough greatly increased, and the most considerable improvement was in Mode 2. The highest final oil recovery of 95.56% was achieved in Mode 2, followed by 90.82% in Mode 3. Mode 1 has the lowest final oil recovery of 74%. The reason is that the increase in supercritical CO_2 and soaking time can make the crude oil fully contact with supercritical CO_2. The decrease in crude oil viscosity and the enhancement of dissolved gas flooding increase final recovery. Gas injection in advance also has an energy enhancement effect on the reservoir. The more gas injection, the more pronounced the energy enhancement effect, the larger the gas swept area, and more increased the original recovery factor (Fan et al., 2020; Gao et al., 2021; Zhao et al., 2015).

Similarly, in Modes 1, 2, and 3, the amount of supercritical CO_2 consumed is 2.01, 1.93, and 1.58 PV, respectively. This shows that adjusting the injection–production system for continuous gas flooding reduces the volume of the injected supercritical CO_2, thereby maximizing the use of injected supercritical CO_2. The variation curve of gas–oil ratio under different injection-production modes is shown in Fig. 6. Mode 1 has the shortest gas channeling time, followed by Mode 3, then Mode 2. The long soaking time of Mode 2 leads to more supercritical CO_2 being dissolved in crude oil in the soaking stage, which can effectively delay the occurrence of gas channeling.

The variation tendency of the injection index under different injection–production modes is shown in Fig. 7. The injection index of each mode in the early stage tends to be the same. Because gas channeling occurs earlier in Mode 1, the injection index rises earlier. The variation tendency of the injection capacity of each mode is consistent with changes in the gas–oil ratio. It is concluded that the injection capacity of supercritical CO_2 is higher in the synchronous injection–production mode. The formation pressure increases and the supercritical CO_2 injection capacity deteriorates with the increase in soaking time.

3.3. Displacement characteristics at different permeability

The influence of core permeability on oil recovery at each stage is shown in Fig. 8. It can be seen from Fig. 8 that the final oil recovery of the rock samples with permeability of 5.1, 2.5, and 0.63 mD are 80%, 75%, and 56.12%, respectively. It can be seen that with the increase in permeability, the recovery factor before gas breakthrough increases, leading to the recovery factor increasing and reaching a specific value. The core with low permeability has a large proportion of tiny pores. In supercritical CO_2 displacement, oil in

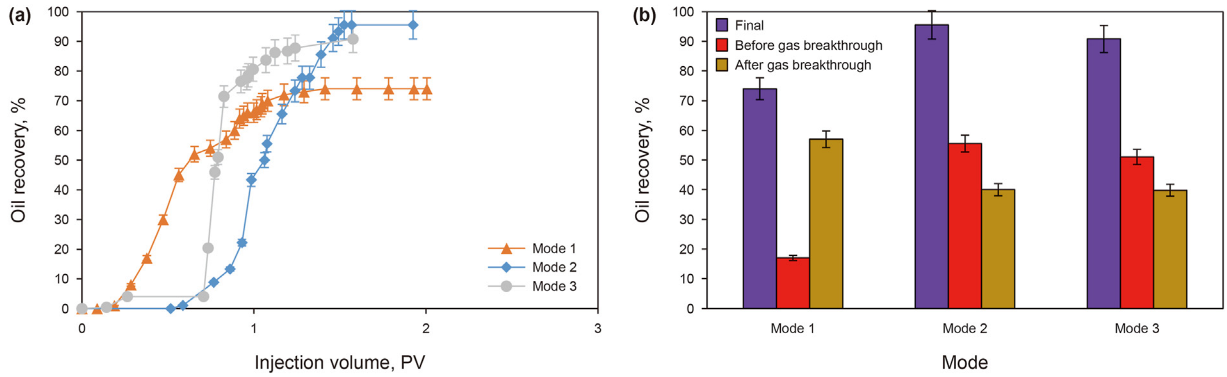

Fig. 5. Relationship between oil recovery and injection volume (**a**) and injection–production modes (**b**).

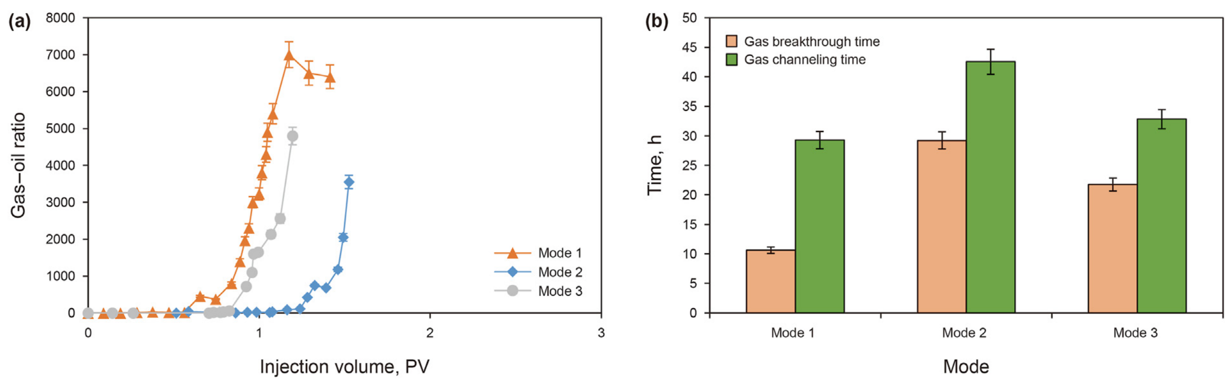

Fig. 6. Curves of gas–oil ratio versus injection volume (**a**), and gas breakthrough time and gas channeling time (**b**) in different injection–production modes.

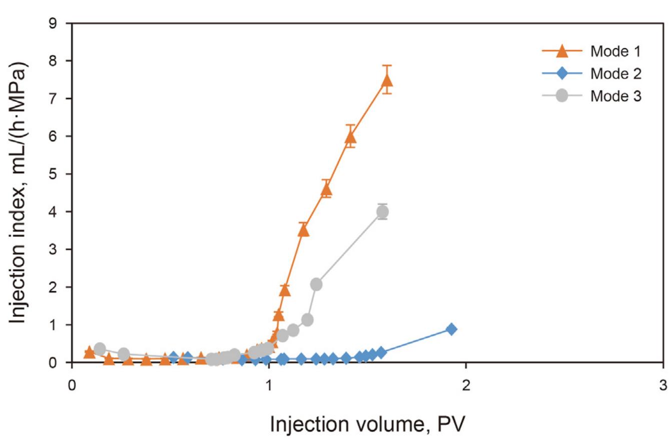

Fig. 7. Comparison of injection index at different injection volumes and injection–production modes.

small pores is challenging to be displaced, resulting in a low recovery rate. Meanwhile, the mixing rate of supercritical CO_2 and crude oil increases with permeability. The higher the permeability is, the more likely it is that the supercritical CO_2 fingering will occur (Niu et al., 2020; Xiao et al., 2017). As shown in Fig. 9, When the core permeability increases further, the gas channeling occurs earlier. The low-permeability core has poor percolation capacity and supercritical CO_2 has a low passing rate, so the gas–oil ratio rises slowly. The gas diffusion rate also changes with the change of permeability. When the permeability is below a specific value, the diffusion rate is minimal with little difference. When the permeability increases to a particular value, the gas diffusion rate rises rapidly. Therefore, both gas breakthrough time and gas channeling time shorten with the increase in core permeability, and the latter shortens more sharply with the increase in permeability (Amarasinghe et al., 2020).

The variation tendency of the injection index of the cores with different permeability is shown in Fig. 10. The core with a permeability of 5.8 mD has a higher injection index and the best injection capacity. The core with a permeability of 0.63 mD tends to be stable. The rapid growth phase of the injection index occurred earlier due to the early occurrence of gas channeling in high-permeability cores. In cores with high permeability, the injection capacity is more significant due to quicker supercritical CO_2 seepage rate.

3.4. Displacement characteristics at different back pressures

The recovery rates at different stages under different back pressures are shown in Fig. 11. By comparing the recovery rates at the early stage of gas injection under different back pressures, it is found that at 10 MPa, the recovery factor before gas channeling is the lowest. With the gas injection, the lower the back pressure, the earlier the gas cut, the earlier the gas channeling, and the lower the final recovery factor. The oil recovery is 81.9%, 87%, and 91%, respectively, at a back pressure of 10, 20, and 30 MPa. Due to the slow dissolution rate of CO_2 and crude oil, the degree of mutual dissolution of oil and gas is low, promoting gas channeling and lower final recovery. At high injection pressure, most of the injected supercritical CO_2 can be diffused to the original stagnant area to replace crude oil to increase production. At the same time, increasing pressure can enhance the miscibility of supercritical CO_2 and crude oil and change the wettability of rock to improve oil

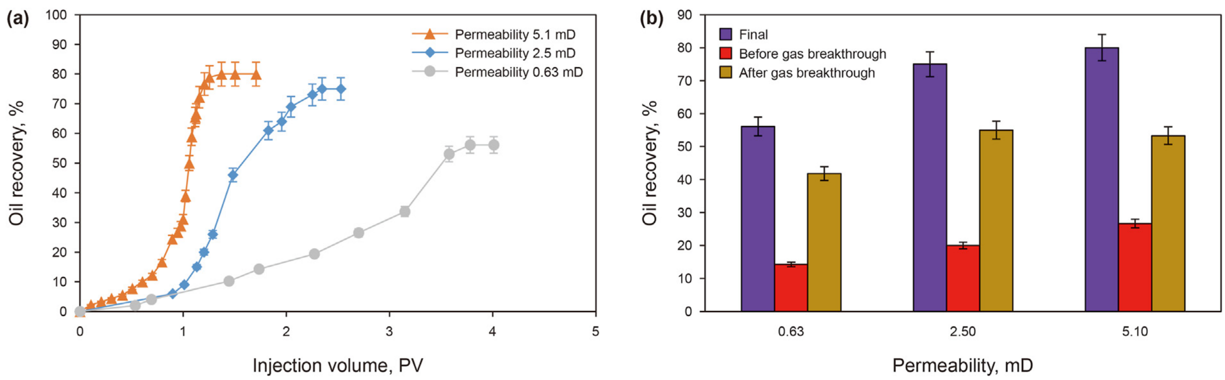

Fig. 8. Relationship between oil recovery and injection volume (**a**) and permeability (**b**).

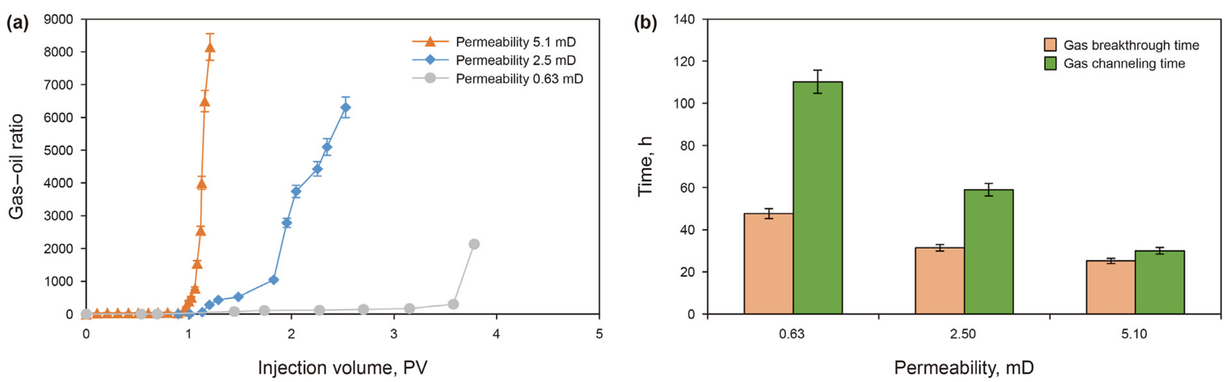

Fig. 9. Curves of gas–oil ratio versus injection volume (**a**), and gas breakthrough time and gas channeling time (**b**) in different permeability cores.

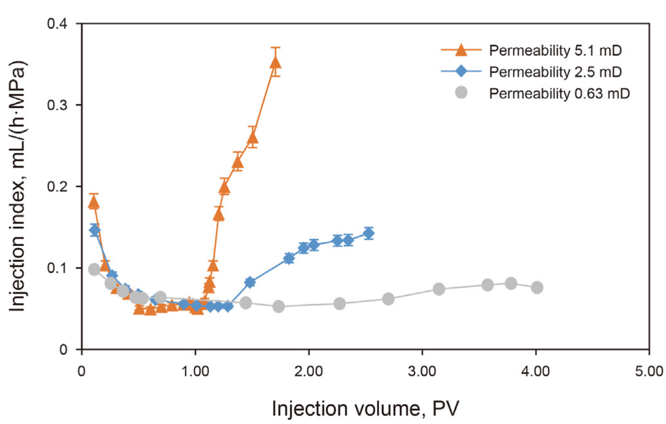

Fig. 10. Comparison of injection index at different injection volumes and permeability.

recovery, which has been mentioned in previous reports (Ding et al., 2017; Du et al., 2018; Lu et al., 2021; Ren et al., 2011). When the pressure reaches above the miscible pressure, the influence of the pressure on the gas channeling time is negligible. Therefore, a reasonable injection pressure should be selected to prolong gas channel time, improve swept volume and oil recovery, and ensure the maximum economic benefit during field test implementation (see Fig. 12).

The variation tendency of the injection index under different back pressures is shown in Fig. 13. The injection index at a back pressure of 10 MPa is larger in the initial gas injection stage. With a back pressure increase during CO_2 injection, the injection index can be reduced to a certain value. The injection capacity is generally better when the back pressure is 10 MPa. The smaller the back pressure, the earlier the gas channeling occurs, resulting in better injection capabilities. At the same time, compared with 10 MPa, the dissolved amount of supercritical CO_2 increases when the back pressure is 30 MPa, which delays the occurrence of gas channeling, resulting in a lower injection index and poor injection capacity.

3.5. Displacement characteristics at different water saturation

In this part, the dry core is saturated with water and oil displacement is followed to establish bound water saturation. Secondly, water flooding is conducted on the oil-bearing cores, and different water saturation is established according to the amount of oil produced. This method simulates gas displacement characteristics at different water flooding stages considering bound water saturation.

Oil recovery at different stages with different water saturation is shown in Fig. 14. The lower the water saturation, the more oil will be displaced in the early stage, resulting in greater displacement efficiency. Gas displacement mainly depends on the carrying effect after gas breakthrough with the increase in water saturation. At a water saturation of 42%, 60%, and 80%, the final oil recovery was 81.05%, 73.44%, and 62.5%, respectively. At high water saturation, oil distribution is relatively dispersed, mostly in tiny pores, resulting in a poorer displacement effect of supercritical CO_2. The presence of water reduces the contact area between oil and CO_2 to a certain extent, reducing the diffusion of CO_2–oil in water-wet pores and making more oil become immovable (Fernø et al., 2015). This shows that when switching to gas injection, the displacement efficiency of supercritical CO_2 is different (Fernø et al., 2015; Torabi and Asghari, 2010). Considering the economic cost of supercritical CO_2, choosing

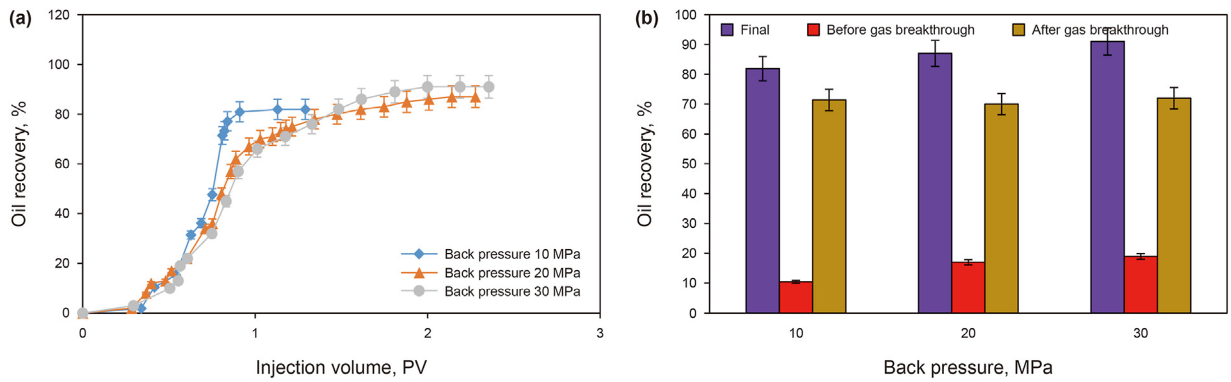

Fig. 11. Relationship between oil recovery and injection volume (**a**) and back pressure (**b**).

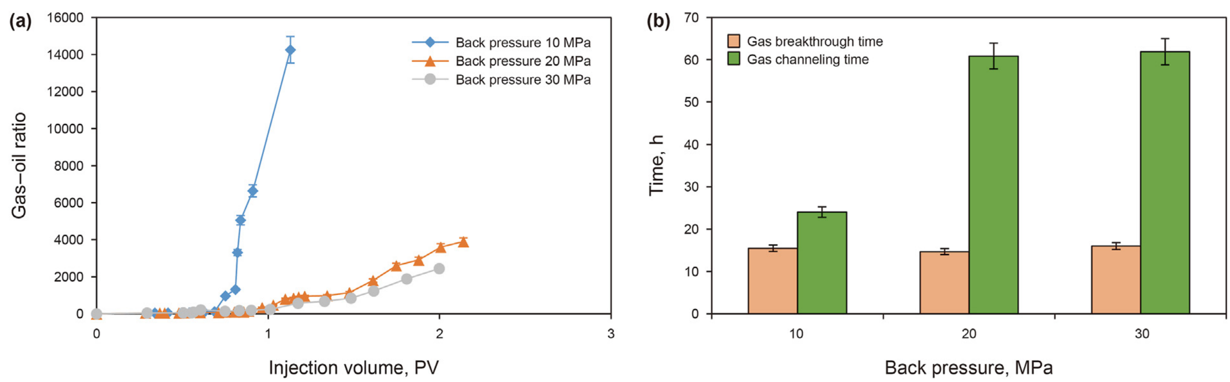

Fig. 12. Curves of gas–oil ratio versus injection volume (**a**), and gas breakthrough time and gas channeling time (**b**) at different back pressures.

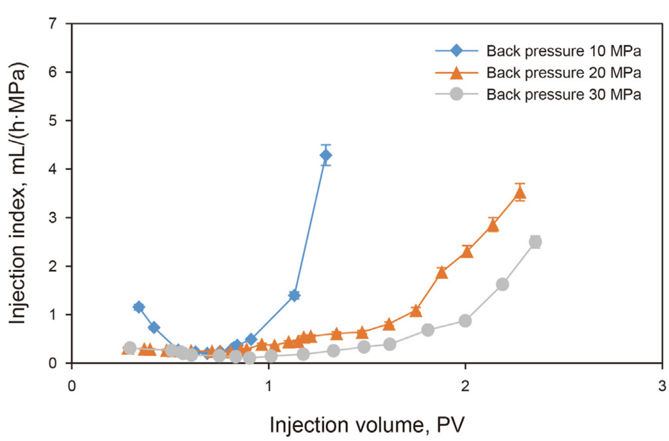

Fig. 13. Comparison of injection index at different injection volumes and back pressures.

the right time for gas injection is very important. Furthermore, when the water saturation increases to a certain value, the water content in the cores is high. At the same time, as shown in Fig. 15, the solubility of supercritical CO_2 in water is small, therefore the gas drive front is easy to break through, causing a reduction in gas breakthrough and gas channeling time. Previous studies in the literature have also confirmed the reduction in gas breakthrough and gas channeling time (Li and Yu, 2020), proving the reliability of the experimental study.

The variation tendency of the injection index under different water saturations is shown in Fig. 16. In the early stage of gas injection, the injection index is also different due to the difference in water saturation. In gas flooding with different water saturation, the injection index of high water saturation is larger than that of low water saturation, so the injection capacity of high water saturation is better. Due to the small amount of supercritical CO_2 dissolved in water, the supercritical CO_2 has a strong piston displacement effect. The liquid and gas at the outlet are observed earlier to maintain the injection capacity at a reasonable level. However, the gas–oil ratio rises faster for cores with low water saturation gas channeling, resulting in better supercritical CO_2 injection capacity and a more extensive injection index. In general, the supercritical CO_2 injection capacity under high water saturation in the early stage of gas injection is better. Still, the supercritical CO_2 injection capacity under low water saturation in the later gas injection stage is better.

4. Conclusions

(1) The gas breakthrough stage is where the oil production rate increases the fastest, however, the injection capacity at this stage is poor. The occurrence of gas channeling produces less oil, a sharp rise in the injection index, and better injection capacity.

(2) With an increase in the gas injection rate, the core pressure increases. At the same time, the dissolution and mixing of CO_2 with crude oil are enhanced. Moreover, the sweep efficiency of injected gas is improved, leading to a higher final recovery factor and a higher supercritical CO_2 consumption. The increase in injection rate delays the occurrence of gas channeling to an extent, but there is an optimal range of increase in injection rate. Adopting a high injection speed

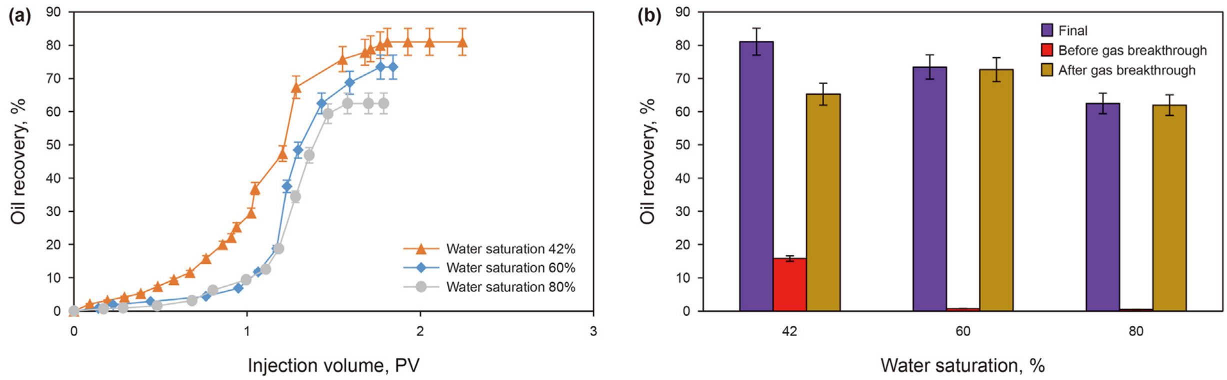

Fig. 14. Relationship between oil recovery and injection volume (**a**) and water saturation (**b**).

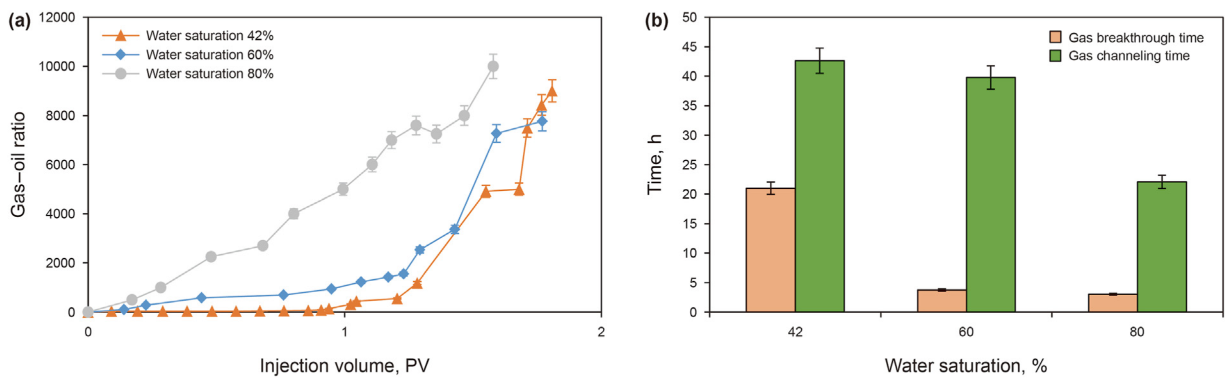

Fig. 15. Curves of gas–oil ratio versus injection volume at different saturation (**a**), and gas breakthrough time and gas channeling time (**b**) at different water saturation.

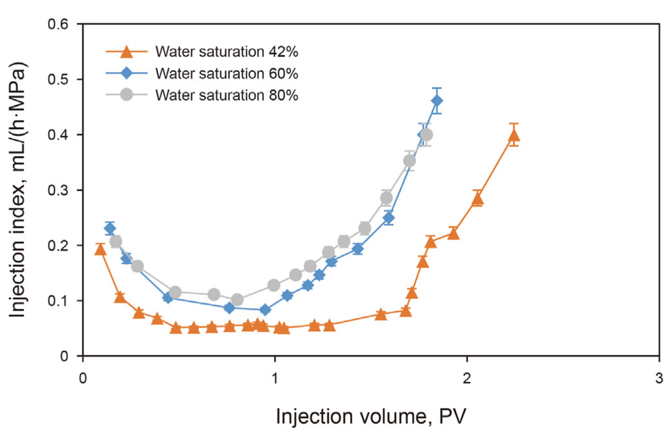

Fig. 16. Comparison of injection index at different injection volumes and water saturation.

will cause the inlet pressure to rise, but this is not a sign of poor injection capacity. At this stage, it is necessary to evaluate the injection capacity quantitatively.

(3) CGI has low displacement efficiency, early gas channeling, more supercritical CO_2 consumption, and better injection capabilities. The AIP mode maximizes the use of supercritical CO_2, improves the energy enhancement effect, expands the spread area of supercritical CO_2, and improves oil recovery, but the injection-production capacity is poor.

(4) The high-permeability core has few tiny pores, and the diffusion rate of supercritical CO_2 is fast. Supercritical CO_2 produces most crude oil in large pores with high recovery and good injection capacity. Similarly, the solubility of supercritical CO_2 and crude oil is high under high pressure, changing the wettability of rock and improving crude oil recovery. The high-pressure gas injection contributes to late gas channeling time and poor injection capacity.

(5) The presence of water reduces the contact between supercritical CO_2 and crude oil under the condition of high water saturation. It reduces the diffusion of the CO_2–crude oil mixture system, resulting in low supercritical CO_2 recovery, early gas invasion time, and good injection capacity. The gas–oil ratio with low water saturation rises sharply after gas channeling, but the injection capacity is adequately controlled and improved. Therefore, it is crucial to choose the appropriate gas injection occasion in the different stages of water flooding.

Declaration of competing interest

The authors declare no competing financial interest.

Acknowledgments

The authors would like to acknowledge financial support from the National Natural Science Foundation of China (No. 51904324, 51974348, U19B6003). The authors are grateful for Shengli Oilfield, providing rock and fluid data for our study.

References

Ajoma, E., Sungkachart, T., Le-Hussain, F., 2021. Effect of miscibility and injection rate on water-saturated CO_2 Injection. Energy 217, 119391. https://doi.org/10.1016/j.energy.2020.119391.

Al-Bayati, D., Saeedi, A., Myers, M., White, C., Xie, Q., 2019. An experimental investigation of immiscible-CO_2-flooding efficiency in sandstone reservoirs: influence of permeability heterogeneity. SPE Reservoir Eval. Eng. 22 (3), 990–997. https://doi.org/10.2118/190876-PA.

Amarasinghe, W., Fjelde, I., Rydland, J.-Å., Guo, Y., 2020. Effects of permeability on CO_2 dissolution and convection at reservoir temperature and pressure conditions: a visualization study. Int. J. Greenh. Gas Control 99, 103082. https://doi.org/10.1016/j.ijggc.2020.103082.

Bikkina, P., Wan, J., Kim, Y., Kneafsey, T.J., Tokunaga, T.K., 2016. Influence of wettability and permeability heterogeneity on miscible CO_2 flooding efficiency. Fuel 166, 219–226. https://doi.org/10.1016/j.fuel.2015.10.090.

Chen, J., Li, T., Wu, S., 2018. Influence of pressure and CO_2 content on the asphaltene precipitation and oil recovery during CO_2 flooding. Petrol. Sci. Technol. 36 (8), 577–582. https://doi.org/10.1080/10916466.2018.1430154.

Chen, S., Liu, Y., Zhang, J., et al., 2021. Formation conditions and evolution of fractures in multiple tight rocks: implications for unconventional reservoir exploitation. J. Petrol. Sci. Eng. 200, 108354. https://doi.org/10.1016/j.petrol.2021.108354.

Cheng, Q., Li, Z., Zhu, G., Zhang, H., 2017. Research and application of CO_2 flooding enhanced oil recovery in low permeability oilfield. Open J. Geol. 7 (9), 1435–1440. https://doi.org/10.4236/ojg.2017.79095.

Cui, M., Ding, Y., Yang, Z., et al., 2011. Numerical simulation study on CO_2 flooding in ultra-low permeability reservoirs. Procedia Environmental Sciences 11, 1469–1472. https://doi.org/10.1016/j.proenv.2011.12.221.

Ding, M., Yuan, F., Wang, Y., et al., 2017. Oil recovery from a CO_2 injection in heterogeneous reservoirs: the influence of permeability heterogeneity, CO_2-oil miscibility and injection pattern. J. Nat. Gas Sci. Eng. 44, 140–149. https://doi.org/10.1016/j.jngse.2017.04.015.

Dong, K., Jiang, M., Li, J., Zhang, D., 2020. Research progresses in formation mechanism of complex fracture network for unconventional reservoir. Arabian J. Geosci. 13 (15), 1–10. https://doi.org/10.1007/s12517-020-05724-w.

Du, X., Gu, M., Duan, S., Xian, X., 2018. The influences of CO_2 injection pressure on CO_2 dispersion and the mechanism of CO_2–CH_4 displacement in shale. J. Energy Resour. Technol. 140 (1). https://doi.org/10.1115/1.4037687.

Fan, J., Zhao, J., He, Y., et al., 2015. Optimization of horizontal well injection-production parameters for ultra-low permeable–tight oil production: a case from Changqing Oilfield, Ordos Basin, NW China. Petrol. Explor. Dev. 42 (1), 74–82. https://doi.org/10.1016/S1876-3804(15)60008-8.

Fan, L., Li, L., Su, Y., et al., 2020. CO_2-prepad injection EOR simulation and sensitivity analysis considering miscibility and geomechanics in tight oil reservoirs. J. Petrol. Sci. Eng. 195, 107905. https://doi.org/10.1016/j.petrol.2020.107905.

Fang, T., Wang, M., Gao, Y., et al., 2019a. Enhanced oil recovery with CO_2/N_2 slug in low permeability reservoir: molecular dynamics simulation. Chem. Eng. Sci. 197, 204–211. https://doi.org/10.1016/j.ces.2018.12.016.

Fang, Y., Yang, E., Yin, D., Gan, Y., 2019b. Study on distribution characteristics of microscopic residual oil in low permeability reservoirs. J. Dispersion Sci. Technol. https://doi.org/10.1080/01932691.2019.1594886.

Fernø, M., Steinsbø, M., Eide, Ø., et al., 2015. Parametric study of oil recovery during CO_2 injections in fractured chalk: influence of fracture permeability, diffusion length and water saturation. J. Nat. Gas Sci. Eng. 27, 1063–1073. https://doi.org/10.1016/j.jngse.2015.09.052.

Gao, S., Yang, Y., Liao, G., et al., 2021. Experimental research on inter-fracture asynchronous injection-production cycle for a horizontal well in a tight oil reservoir. J. Petrol. Sci. Eng. https://doi.org/10.1016/j.petrol.2021.109647, 109647.

Han, J., Lee, M., Lee, W., Lee, Y., Sung, W., 2016. Effect of gravity segregation on CO_2 sequestration and oil production during CO_2 flooding. Appl. Energy 161, 85–91. https://doi.org/10.1016/j.apenergy.2015.10.021.

He, D., Jiang, P., Xu, R., 2019. Pore-scale experimental investigation of the effect of supercritical CO_2 injection rate and surface wettability on salt precipitation. Environ. Sci. Technol. 53 (24), 14744–14751. https://doi.org/10.1021/acs.est.9b03323.

Hu, W., Wei, Y., Bao, J., 2018. Development of the theory and technology for low permeability reservoirs in China. Petrol. Explor. Dev. 45 (4), 685–697. https://doi.org/10.1016/S1876-3804(18)30072-7.

Li, Y., Yu, Q., 2020. Rock-core scale modeling of initial water saturation effects on CO_2 breakthrough pressure in CO_2 geo-sequestration. J. Hydrol. 580, 124234. https://doi.org/10.1016/j.jhydrol.2019.124234.

Li, M., Shan, W., Liu, X., Shang, G., 2006. Laboratory study on miscible oil displacement mechanism of supercritical carbon dioxide. Acta Pet. Sin. 2006 (3), 80–83 (in Chinese) doi:CNKI:SUN:SYXB.0.2006-03-017.

Li, A., Ren, X., Fu, S., et al., 2018. The experimental study on the flooding regularities of various CO_2 flooding modes implemented on ultralow permeability cores. J. Energy Resour. Technol. 140 (7). https://doi.org/10.1115/1.4039319.

Li, C., Maggi, F., Zhang, K., et al., 2019a. Effects of variable injection rate on reservoir responses and implications for CO_2 storage in saline aquifers. Greenhouse Gases: Sci. Technol. 9 (4), 652–671. https://doi.org/10.1002/ghg.1888.

Li, L., Wang, C., Li, D., et al., 2019b. Experimental investigation of shale oil recovery from Qianjiang core samples by the CO_2 huff-n-puff EOR method. RSC Adv. 9 (49), 28857–28869. https://doi.org/10.1039/C9RA05347F.

Liu, H., Valocchi, A.J., Werth, C., Kang, Q., Oostrom, M., 2014. Pore-scale simulation of liquid CO_2 displacement of water using a two-phase lattice Boltzmann model. Adv. Water Resour. 73, 144–158. https://doi.org/10.1016/j.advwatres.2014.07.010.

Liu, H., Zhu, Z., Patrick, W., et al., 2020. Numerical visualization of supercritical CO_2 displacement in pore-scale porous and fractured media saturated with water. Advances in Geo-Energy Research 4 (4), 419–434. https://doi.org/10.46690/ager.2020.04.07.

Lu, Y., Tian, R., Tang, J., et al., 2021. Investigating the mineralogical and chemical effects of CO_2 injection on shale wettability at different reservoir temperatures and pressures. Energy Fuel. 35 (18), 14838–14851. https://doi.org/10.1021/acs.energyfuels.1c01943.

Mahabadi, N., Paassen, L., Battiato, I., et al., 2020. Impact of pore-scale characteristics on immiscible fluid displacement. Geofluids, doi:10.1155/2020/5759023.

Matkivskyi, S., Kondrat, O., Burachok, O., 2021. Investigation of the influence of the carbon dioxide (CO_2) injection rate on the activity of the water pressure system during gas condensate fields development. E3S Web of Conferences 230, 1011. https://doi.org/10.1051/e3sconf/202123001011.

Niu, Q., Cao, L., Sang, S., et al., 2020. Study on the anisotropic permeability in different rank coals under influences of supercritical CO_2 adsorption and effective stress and its enlightenment for CO_2 enhance coalbed methane recovery. Fuel 262, 116515. https://doi.org/10.1016/j.fuel.2019.116515.

Park, H., Jiang, L., Kiyama, T., et al., 2017. Influence of sedimentation heterogeneity on CO_2 flooding. Energy Proc. 114, 2933–2941.

Pei, Y., Zhou, H., Li, D., et al., 2020. A novel unconventional reservoir fracturing method-liquid self-propping fracturing technology. International Petroleum Technology Conference.

Qian, K., Yang, S., Dou, H., Zhang, J., 2020. Microscopic characteristics of oil displacement with different CO_2 injection modes in extra-low permeability reservoirs. Xinjiang Pet. Geol. 41 (2), 204–208. https://doi.org/10.7657/XJPG20200211 (in Chinese).

Ren, B., Xu, Y., Niu, B., et al., 2011. Laboratory assessment and field pilot of near miscible CO_2 injection for IOR and storage in a tight oil reservoir of Shengli Oilfield, China. SPE Enhanced Oil Recovery Conference, doi:10.2118/144108-MS.

Sander, R., Pan, Z., Connell, L.D., 2017. Laboratory measurement of low permeability unconventional gas reservoir rocks: a review of experimental methods. J. Nat. Gas Sci. Eng. 37, 248–279. https://doi.org/10.1016/j.jngse.2016.11.041.

Shen, H., Yang, Z., Li, X., et al., 2021. CO_2-responsive agent for restraining gas channeling during CO_2 flooding in low permeability reservoirs. Fuel 292, 120306. https://doi.org/10.1016/j.fuel.2021.120306.

Shi, Y., Jia, Y., Pan, W., et al., 2017. Potential evaluation on CO_2-EGR in tight and low-permeability reservoirs. Nat. Gas. Ind. B 4 (4), 311–318. https://doi.org/10.1016/j.ngib.2017.08.013.

Sun, Y., Li, Q., Yang, D., Liu, X., 2016. Laboratory core flooding experimental systems for CO_2 geosequestration: an updated review over the past decade. Journal of Rock Mechanics and Geotechnical Engineering 8 (1), 113–126.

Torabi, F., Asghari, K., 2010. Effect of operating pressure, matrix permeability and connate water saturation on performance of CO_2 huff-and-puff process in matrix-fracture experimental model. Fuel 89 (10), 2985–2990. https://doi.org/10.1016/j.fuel.2010.05.020.

Wang, R., Lv, C., Lun, Z., et al., 2011. Study on gas channeling characteristics and suppression methods in CO_2 flooding for low permeability reservoirs. SPE Asia Pacific Oil and Gas Conference and Exhibition. https://doi.org/10.2118/142306-MS.

Wang, H., Liao, X., Dou, X., et al., 2014. Potential evaluation of CO_2 sequestration and enhanced oil recovery of low permeability reservoir in the Junggar Basin, China. Energy Fuel. 28 (5), 3281–3291. https://doi.org/10.1021/ef4025068.

Wang, S., Chen, C., Shiau, B., Harwell, J.H., 2018. In-situ CO_2 generation for EOR by using urea as a gas generation agent. Fuel 217, 499–507. https://doi.org/10.1016/j.fuel.2017.12.103.

Wang, J., Zhou, F., Fan, F., Zhang, L., Yao, E., 2019. Study on the influence of CO_2 finger-channeling flooding on oil displacement efficiency and anti-channeling method. ARMA-CUPB Geothermal International Conference. American Rock Mechanics Association. In: https://onepetro.org/ARMACUPB/proceedings-abstract/CUPB19/All-CUPB19/ARMA-CUPB-19-3861/125230.

Wang, Y., Shang, Q., Zhou, L., Jiao, Z., 2021. Utilizing macroscopic areal permeability heterogeneity to enhance the effect of CO_2 flooding in tight sandstone reservoirs in the Ordos Basin. J. Petrol. Sci. Eng. 196, 107633. https://doi.org/10.1016/j.petrol.2020.107633.

Wei, N., Gill, M., Crandall, D., et al., 2014. CO_2 flooding properties of Liujiagou sandstone: influence of sub-core scale structure heterogeneity. Greenhouse Gases: Sci. Technol. 4 (3), 400–418. https://doi.org/10.1002/ghg.1407.

Wei, J., Zhou, J., Li, J., et al., 2021. Experimental study on oil recovery mechanism of CO_2 associated enhancing oil recovery methods in low permeability reservoirs. J. Petrol. Sci. Eng. 197, 108047. https://doi.org/10.1016/j.petrol.2020.108047.

Xiao, P., Yang, Z., Wang, X., Xiao, H., Wang, X., 2017. Experimental investigation on CO_2 injection in the Daqing extra/ultra-low permeability reservoir. J. Petrol. Sci. Eng. 149, 765–771. https://doi.org/10.1016/j.petrol.2016.11.020.

Xiong, J., Liu, X., Liang, L., 2015. Experimental study on the pore structure characteristics of the Upper Ordovician Wufeng Formation shale in the southwest portion of the Sichuan Basin, China. J. Nat. Gas Sci. Eng. 22, 530–539. https://doi.org/10.1016/j.jngse.2015.01.004.

Xu, L., Li, Q., Myers, M., et al., 2020. The effects of porosity and permeability changes on simulated supercritical CO_2 migration front in tight glutenite under different effective confining pressures from 1.5 MPa to 21.5 MPa. Greenhouse Gases:

Science and Technology. https://doi.org/10.1002/ghg.2043.
Yamabe, H., Tsuji, T., Liang, Y., Matsuoka, T., 2015. Lattice Boltzmann simulations of supercritical CO_2–water drainage displacement in porous media: CO_2 saturation and displacement mechanism. Environ. Sci. Technol. 49 (1), 537–543. https://doi.org/10.1021/es504510y.
Zhang, L., Zhao, F.L., Hou, J.R., 2012. Experimental study of improving the CO_2 flooding development effect in ultra-low permeability reservoir. Advanced Materials Research. Trans Tech Publ, pp. 2470–2474. https://doi.org/10.4028/www.scientific.net/AMR.594-597.2470.
Zhang, J., Zhang, H.X., Ma, L.Y., Liu, Y., Zhang, L., 2020. Performance evaluation and mechanism with different CO_2 flooding modes in tight oil reservoir with fractures. J. Petrol. Sci. Eng. 188, 106950. https://doi.org/10.1016/j.petrol.2020.106950.
Zhao, F., Hao, H., Hou, J., Hou, L., Song, Z., 2015. CO_2 mobility control and sweep efficiency improvement using starch gel or ethylenediamine in ultra-low permeability oil layers with different types of heterogeneity. J. Petrol. Sci. Eng. 133, 52–65. https://doi.org/10.1016/j.petrol.2015.05.014.
Zhao, F., Wang, P., Huang, S., et al., 2020a. Performance and applicable limits of multi-stage gas channeling control system for CO_2 flooding in ultra-low permeability reservoirs. J. Petrol. Sci. Eng. 192, 107336. https://doi.org/10.1016/j.petrol.2020.107336.
Zhao, Y., Zhang, Y., Lei, X., Zhang, Y., Song, Y., 2020b. CO_2 flooding enhanced oil recovery evaluated using magnetic resonance imaging technique. Energy 203, 117878. https://doi.org/10.1016/j.energy.2020.117878.
Zhu, Q., Zhou, Q., Li, X., 2016. Numerical simulation of displacement characteristics of CO_2 injected in pore-scale porous media. Journal of Rock Mechanics and Geotechnical Engineering 8 (1), 87–92. https://doi.org/10.1016/j.jrmge.2015.08.004.